



UNIVERSIDAD POLITECNICA  
DE MADRID  
Escuela Técnica Superior de Ingeniería  
Aeronáutica y del Espacio



## Master in Materiales Compuestos

# NUMERICAL SIMULATION TECHNIQUES

## COMPUTER LAB. ABAQUS EXERCISE

Alessandro Federico Acuna Guardia

Madrid, 2024-2025

# Contents

<b>1</b>	<b>Introduction</b>	<b>2</b>
<b>2</b>	<b>Description of the Model</b>	<b>3</b>
2.1	Geometry and Mesh . . . . .	3
2.2	E-Glass UD Material Properties . . . . .	3
2.2.1	Elastic Behaviour in Abaqus . . . . .	4
2.2.2	Damage Initiation: Hashin Criteria . . . . .	5
2.3	Reference System and Stacking Sequence . . . . .	5
2.3.1	Stacking Sequence . . . . .	6
<b>3</b>	<b>Boundary Conditions and Loading</b>	<b>7</b>
3.1	Constraints and Displacement . . . . .	7
3.2	Loading . . . . .	8
3.3	Output Requests . . . . .	8
3.4	Post-Processing: Stress and Strain Calculation . . . . .	9
<b>4</b>	<b>Result</b>	<b>10</b>
4.1	Tensile Loading Results . . . . .	10
4.1.1	Failure Sequence and Interpretation . . . . .	11
4.1.2	Stress–Strain Curve Interpretation . . . . .	12
4.1.3	Failure Mode Summary . . . . .	12
4.2	Compressive Loading Results . . . . .	12
4.2.1	Failure Sequence and Interpretation . . . . .	13
4.2.2	Stress–Strain Curve Interpretation . . . . .	14
4.2.3	Failure Mode Summary . . . . .	14
<b>5</b>	<b>Ratio Analysis</b>	<b>15</b>
5.1	Calculation of Tensile to Compressive Strength Ratio . . . . .	15
5.1.1	Ultimate Strengths . . . . .	15
5.1.2	Strength Ratio Calculation . . . . .	15
5.1.3	Interpretation . . . . .	15
5.2	Conclusion . . . . .	16

# Chapter 1

## Introduction

The objective of this exercise is to analyse the mechanical behaviour of a laminate with the stacking sequence  $[0^\circ, \pm 45^\circ, 0^\circ, 90^\circ]_s$  under tensile and compressive loading, using a damage model based on the Hashin criterion. This type of analysis is crucial in composite materials engineering, as it enables us to understand how the different fiber orientations affect the laminate's mechanical properties and load-carrying capacity.

The main goal, therefore, is to obtain the stress-strain ( $\sigma-\varepsilon$ ) curves of the laminate in both tension and compression, and to determine the ratio between the maximum tensile strength and compressive strength, i.e., the extent to which the laminate can withstand compressive loads compared to tensile loads. Throughout the analysis, a progressive damage procedure is applied: in each *step*, the first ply reaching the damage index (Failure Index) equal to 1 is considered to have failed and is then removed or “deactivated” from the model. In this way, it is possible to reconstruct the *ply-by-ply* failure evolution and, consequently, the entire laminate behaviour up to final collapse.

In summary, this report describes the modelling choices (geometry, mesh, material properties, and boundary conditions) and the *steps* required to compute the critical stress and strain values in tension and compression, ultimately discussing the results obtained with special emphasis on the failure sequence and the damage mechanisms of the composite material.

# Chapter 2

## Description of the Model

### 2.1 Geometry and Mesh

The analysed specimen is a rectangular composite laminate coupon with a length of  $L = 100\text{ mm}$  and a width of  $B = 20\text{ mm}$ . It is composed of ten unidirectional (UD) plies, each with a thickness of  $0.25\text{ mm}$ , resulting in a total laminate thickness of  $2.5\text{ mm}$ . The specimen is composed by free lateral edges and is subjected to loading (tension or compression) along its shorter edges.

The finite element model employs shell elements of type S4R—a 4-node, doubly-curved, reduced integration shell element with hourglass control. These elements are particularly suitable for thin composite laminates, as they allow for efficient definition of ply orientations without requiring multiple elements through the thickness.

The mesh is structured and consists of quadrilateral elements with a characteristic element size of  $2\text{ mm}$ , as illustrated in Figure 2.1.

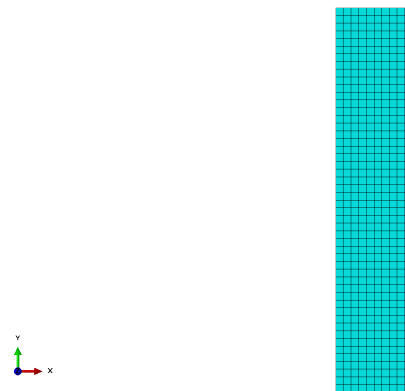


Figure 2.1: Representative finite element mesh of the E-Glass UD laminate coupon.

### 2.2 E-Glass UD Material Properties

The composite material used in this analysis is an E-Glass Unidirectional (UD) laminate. The elastic properties and strength parameters used in the simulation include Young's modulus, Poisson's ratio, shear modulus, and the ultimate strengths in both longitudinal and transverse directions, as well as in-plane shear strength. These parameters are listed in Table 2.1.

**Note:** In this context, the **longitudinal direction** refers to the fiber orientation at  $0^\circ$  with respect to the local coordinate system of the ply, while the **transverse direction**

corresponds to  $90^\circ$ .

- $\sigma_l, \sigma_t$ : Ultimate strengths [MPa] in the longitudinal ( $l$ ) and transverse ( $t$ ) directions;
- $E_l, E_t$ : Young's modulus [GPa] in the  $l$  and  $t$  directions;
- $\nu_{LT}$ : Poisson's ratio;
- $\sigma_{lt}$ : In-plane shear strength [MPa];
- $G_{lt}$ : In-plane shear modulus [GPa].

Parameter	Tension	Compression	In-Plane Shear
$\sigma_l$ [MPa]	1100	900	—
$\sigma_t$ [MPa]	35	150	—
$E_l$ [GPa]	43	42	—
$E_t$ [GPa]	8	10	—
$\nu_{LT}$ [-]	0.28	0.28	—
$\sigma_{lt}$ [MPa]	—	—	60
$G_{lt}$ [GPa]	—	—	4

Table 2.1: Mechanical properties of the E-Glass UD composite material.

### 2.2.1 Elastic Behaviour in Abaqus

The elastic properties were defined in Abaqus using:

*Material* → *Mechanical* → *Elastic* → *Lamina*

The following parameters were specified:  $E_1$ ,  $E_2$ ,  $\nu_{12}$ ,  $G_{12}$ ,  $G_{13}$ , and  $G_{23}$ , according to the material data sheet. See Figure 2.2 for the Abaqus interface.

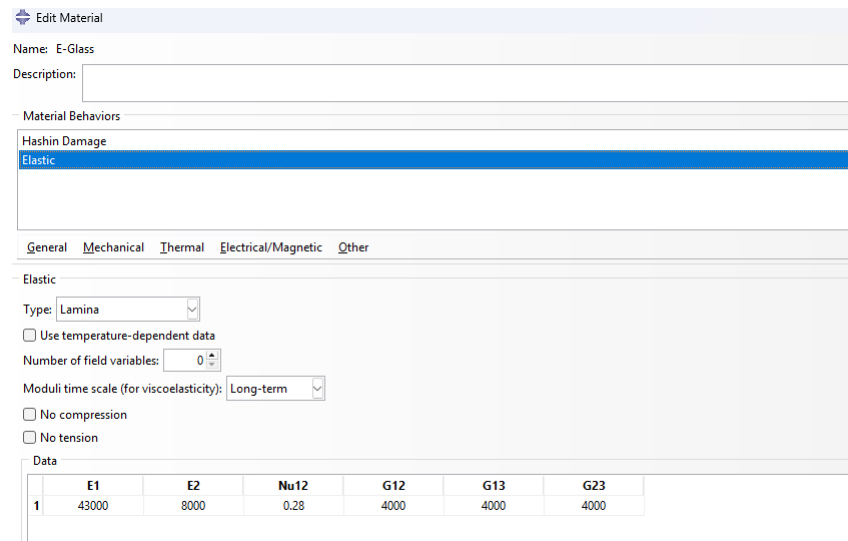


Figure 2.2: Definition of E-Glass UD elastic properties in Abaqus.

## 2.2.2 Damage Initiation: Hashin Criteria

The failure behaviour was modeled using the Hashin damage initiation criteria, enabled via:

*Damage for Fiber-Reinforced Composites → Hashin*

The required input parameters were:

- $\sigma_l$ : Longitudinal tensile and compressive strength;
- $\sigma_t$ : Transverse tensile and compressive strength;
- $\sigma_{lt}$ : In-plane shear strength.

An example from Abaqus is shown in Figure 2.3. The Hashin model distinguishes between fiber and matrix failure, both under tensile and compressive loading. Damage initiates when the failure index of any failure mode reaches 1.

In this study, no damage evolution (i.e., progressive degradation of stiffness) was included.

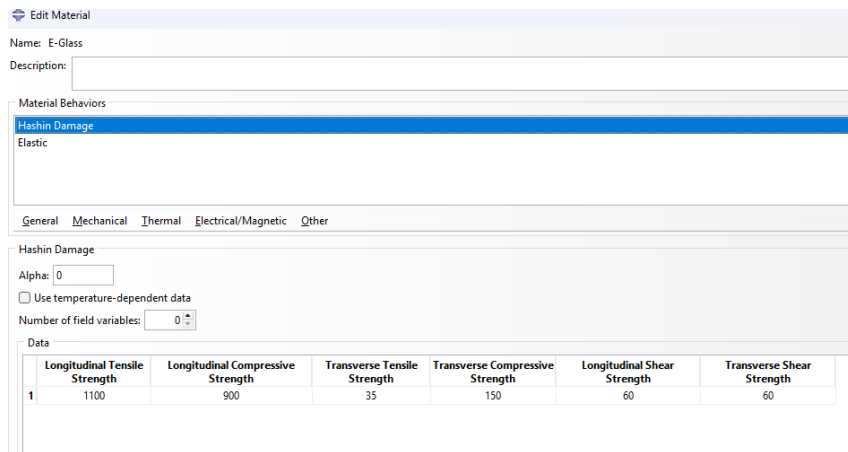


Figure 2.3: Definition of Hashin damage initiation criteria in Abaqus for E-Glass UD.

## 2.3 Reference System and Stacking Sequence

Since the specimen in the assignment was rotated by 90° counter-clockwise with respect to the global coordinate system of Abaqus, a local reference system was created to correctly assign fiber orientations. This new red system is shown in Figure 2.4.

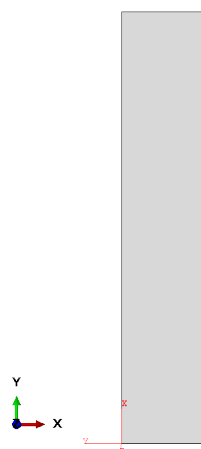


Figure 2.4: Local reference red system used for fiber orientation definition.

### 2.3.1 Stacking Sequence

The laminate follows a symmetric stacking sequence:

$$[0^\circ, \pm 45^\circ, 0^\circ, 90^\circ]_s$$

This sequence contains five unique ply orientations, mirrored respect to the mid-plane, resulting in a total of ten plies. Each ply is 0.25 mm thick, for a total laminate thickness of 2.5 mm.

- **Ply orientations:** The upper half of the laminate consists of  $0^\circ$ ,  $+45^\circ$ ,  $-45^\circ$ ,  $0^\circ$ , and  $90^\circ$  plies. The lower half mirrors this to ensure symmetry. This configuration eliminates bending-extension coupling and keeps the mid-plane as a neutral axis during in-plane loading.
- **Implementation in Abaqus:** The composite layup was created using the *Layup Manager* in Abaqus/CAE. Each ply was assigned a specific orientation relative to the newly defined local system. The  $\pm 45^\circ$  plies were entered as separate layers. All plies had the same thickness of 0.25 mm.

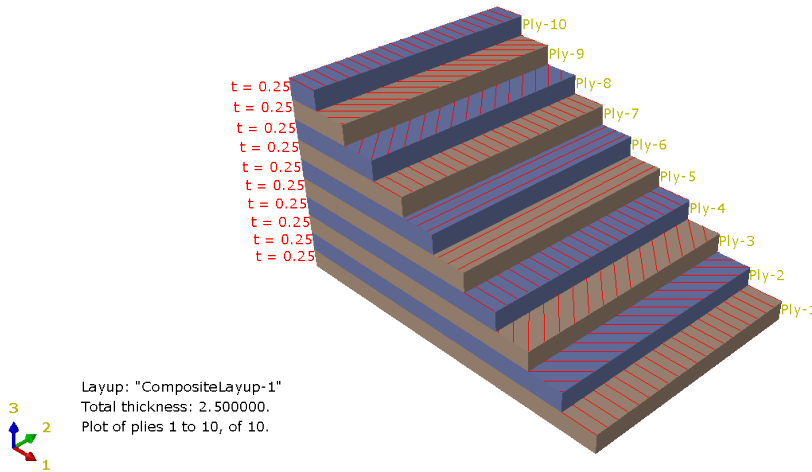


Figure 2.5: Schematic illustration of the  $[0^\circ, \pm 45^\circ, 0^\circ, 90^\circ]_s$  stacking sequence.

# Chapter 3

## Boundary Conditions and Loading

### 3.1 Constraints and Displacement

The bottom edge of the specimen was fully constrained using a clamped boundary condition, where all translational and rotational degrees of freedom (U1, U2, U3, UR1, UR2, UR3) were set to zero. To impose displacement on the top edge, a *Reference Point* (RP) was defined and coupled to the top edge using a *kinematic coupling constraint* (via an **Equation or Coupling** interaction in Abaqus), ensuring that the motion of the entire edge is governed by the RP's degrees of freedom.

This constraint enforces the following kinematic relations:

- TOPEDGE:DOF1 = RP:DOF1
- TOPEDGE:DOF2 = RP:DOF2
- TOPEDGE:DOF3 = RP:DOF3

In this setup, a displacement imposed at the RP causes a uniform displacement of the entire top edge, allowing for accurate simulation of tensile or compressive loading by varying the sign of the imposed displacement in the vertical (*Y*) direction.

Figure 3.1 shows the model configuration for a case where a positive displacement is applied along the *Y* direction, corresponding to a uniaxial tensile test.

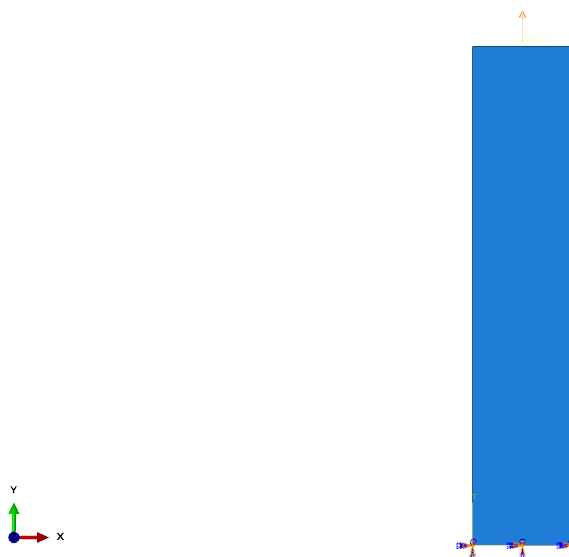


Figure 3.1: Model setup: applied boundary conditions and displacement loading.

## 3.2 Loading

While the clamped boundary condition was applied in the initial step, the mechanical loading was introduced using a **displacement-controlled** approach.

A prescribed vertical displacement was applied at a *Reference Point (RP)*, which was kinematically coupled to the top edge of the structure.

The loading was implemented through a single *Static, General* analysis step, configured as follows:

- **Time period:** 10
- **Maximum number of increments:** 1000
- **Increment sizes:**
  - **Initial:** 0.1
  - **Minimum:** 0.01
  - **Maximum:** 0.1

This configuration ensures a gradual and stable application of the prescribed displacement. The relatively small initial increment (0.1 compared to the total time of 10) allows for finer control during the early stages of the analysis, which is particularly important for capturing the onset of nonlinear behaviour or material degradation.

The minimum increment size (0.01) enables the solver to automatically reduce the step size in regions of high nonlinearity or convergence difficulty. Instead, the maximum increment size (0.1) prevents abrupt load changes that could hinder convergence or reduce numerical accuracy.

After the displacement is applied, the analysis identifies the frame in which any failure criterion is met (when the failure index exceeds 1).

At that point, the corresponding ply is determined, and the associated **reaction force** and **displacement** are extracted for further evaluation.

## 3.3 Output Requests

To monitor failure initiation, a *Field Output Request* was defined with the entire composite layup as the domain. The following output variables were selected to track damage initiation based on the Hashin failure theory:

- **HSNFTCRT** – Fiber tensile damage initiation
- **HSNFCCRT** – Fiber compressive damage initiation
- **HSNMTCRT** – Matrix tensile damage initiation
- **HSNMCCRT** – Matrix compressive damage initiation

The output at section points was set to the middle of each ply. This allows capturing internal damage initiation across the layup thickness without biasing results toward surface effects (as could happen by using only top or bottom). This is particularly useful for identifying the first ply failure, which often occurs internally in composites due to matrix cracking or interlaminar stresses.

Once the failed ply and the corresponding frame are identified, that ply is deactivated in the composite layup. This enables a subsequent simulation to be performed with a higher applied load and the previously failed ply excluded, allowing the detection of the next failure event in the sequence.

Additionally, a *History Output Request* was used to extract the global response quantities:

- **U2:** Displacement in the loading direction (Y-axis)
- **RF2:** Reaction force along the Y-axis

Unlike the field output, the history output was applied not to the composite layup, but specifically to the **Reference Point (RP)**.

Since the RP is kinematically coupled to the top edge, it captures the global displacement and reaction force, enabling the computation of engineering stress and strain.

### 3.4 Post-Processing: Stress and Strain Calculation

From the output data, the engineering strain and stress were computed using the following relations:

$$\varepsilon = \frac{\delta L}{L_0}$$

$$\sigma = \frac{F}{A} \quad [\text{MPa}]$$

Where:

- $\delta L$  = imposed vertical displacement [mm], extracted from U2 at the RP
- $L_0$  = initial length of the specimen [mm]
- $F$  = reaction force at the RP in the Y-direction (RF2) [N]
- $A$  = cross-sectional area of the specimen [ $\text{mm}^2$ ]

In this study,  $L_0 = 100$  mm and  $A = 5 \text{ mm}^2$ .

These values were used to plot the stress-strain curve and to identify the load level at which the first ply failure occurs, as indicated by the Hashin damage criteria.

# Chapter 4

## Result

### 4.1 Tensile Loading Results

The results obtained from the tensile loading simulation are summarized in Table 4.1. In this simulation, the displacement was applied along the **Y-axis**, which is the axial loading direction for the laminate. This detail is crucial, as it determines the nature of the stress experienced by each ply depending on its fiber orientation. The observed failure modes and their sequence strongly reflect this loading direction.

Ply	Angle	FI	Index FI	Disp. [mm]	Force [N]	$\varepsilon$ [%]	$\sigma$ [MPa]
1	0°	HSNFTCRT	3	2.4	20660	2.40	413
2	+45°	HSNMTCRT	2	0.516	5806	0.52	116
3	-45°	HSNMTCRT	2	0.516	5806	0.52	116
4	0°	HSNFTCRT	3	2.4	20660	2.40	413
5	90°	HSNMTCRT	1	0.405	5037	0.405	101
6	90°	HSNMTCRT	1	0.405	5037	0.405	101
7	0°	HSNFTCRT	3	2.4	20660	2.40	413
8	-45°	HSNMTCRT	2	0.516	5806	0.52	116
9	+45°	HSNMTCRT	2	0.516	5806	0.52	116
10	0°	HSNFTCRT	3	2.4	20660	2.40	413

Table 4.1: Results under tensile loading. FI = Failure Index;  $\varepsilon$  = Strain;  $\sigma$  = Stress.

In Figure 4.1, the failure of ply 5 due to matrix tension is shown as an example. This indicates that in a subsequent simulation with a higher applied displacement, plies 5 and 6 were deactivated in the composite layup as they had already exceeded the failure criterion.

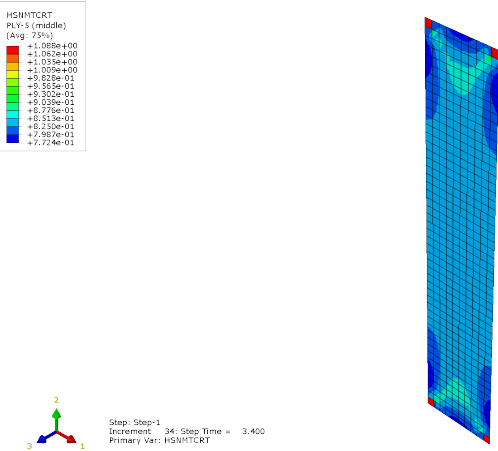


Figure 4.1: Result HSNMTCRT for ply 5.

### 4.1.1 Failure Sequence and Interpretation

Given that the tensile load is applied along the **Y-axis**, the response of each ply is heavily influenced by its fiber orientation:

- **90° plies (Plies 5 and 6):** Fail **first** at low displacement (0.405 mm) and moderate stress (101 MPa). Since the fibers are aligned with the global Y-axis (the loading direction), these plies exhibit higher stiffness in the loading direction. However, the early failure mode observed is matrix tensile cracking (**HSNMTCRT**), which suggests that the failure initiates in the matrix phase rather than in the fibers. This indicates that while the fibers can sustain the load, local matrix micro-cracking or fiber–matrix interface debonding becomes the limiting factor at lower stress levels.
- **±45° plies (Plies 2, 3, 8, 9):** Fail **second** at 0.516 mm displacement and 116 MPa stress. These plies are oriented at ±45° with respect to the loading axis, and thus experience significant in-plane shear when the laminate is loaded in tension. The resulting stress state leads to matrix-dominated failure (**HSNMTCRT**), primarily driven by shear-induced damage mechanisms within the matrix or at the fiber–matrix interface.
- **0° plies (Plies 1, 4, 7, 10):** Fail **last** at 2.4 mm and very high stress (413 MPa). These plies have fibers oriented transverse to the loading direction (Y-axis), meaning the matrix carries most of the load along Y. Nevertheless, under increasing tensile load, these plies eventually reach fiber tensile failure (**HSNFTCRT**). This suggests that local stress redistribution or load transfer from failed plies leads to sufficient axial stress in these off-axis plies to trigger fiber rupture, marking the final catastrophic failure.

### 4.1.2 Stress–Strain Curve Interpretation

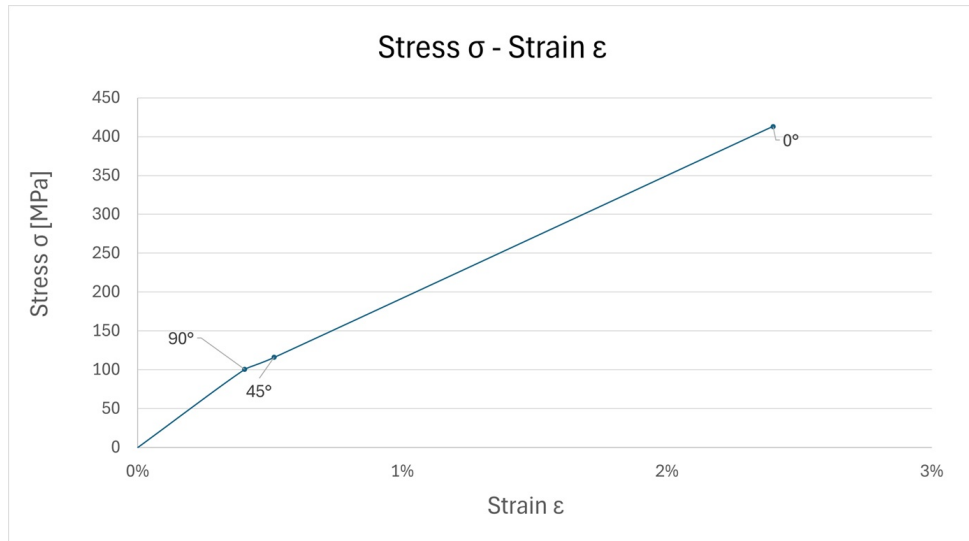


Figure 4.2: Stress–strain curve under tensile loading (Y-axis), with failure stages.

In Figure 4.2, the laminate exhibits a characteristic **stepwise stiffness reduction**, which corresponds to progressive damage:

- **Point 1:** Initial drop from 90° matrix failure.
- **Point 2:** Second drop due to ±45° matrix shear failure.
- **Point 3:** Final steep drop indicating fiber rupture in the 0° plies.

This behaviour confirms a progressive damage mechanism typical of quasi-ductile failure in composite laminates.

### 4.1.3 Failure Mode Summary

The sequence of failures ( $90^\circ \rightarrow \pm 45^\circ \rightarrow 0^\circ$ ) reflects an ideal and safe damage evolution. The initial matrix failures do not cause structural collapse but allow stress redistribution. Final failure via HSNFTCRT confirms that fibers in 0° plies resist until the laminate's ultimate capacity.

The applied Y-axis loading direction is essential in understanding this progression, as it determines which plies are stressed axially, transversely, or in shear.

## 4.2 Compressive Loading Results

The results obtained from the compressive loading simulation are summarized in Table 4.2. In this simulation, the displacement was applied along the **Y-axis**, as in the tensile case, but with opposite sign. This reversal of the loading direction significantly influences the failure modes, as compressive stresses interact differently with the fiber and matrix, particularly in off-axis plies.

Ply	Angle	FI	Index FI	Disp. [mm]	Force [N]	$\varepsilon$ [%]	$\sigma$ [MPa]
1	0°	HSNFCCRT	3	2.0	16819	2.00	336
2	+45°	HSNMCCRT	1	1.1	13281	1.10	265.6
3	-45°	HSNMCCRT	1	1.1	13281	1.10	265.6
4	0°	HSNFCCRT	3	2.0	16819	2.00	336
5	90°	HSNMCCRT	2	1.4	13293	1.40	265.9
6	90°	HSNMCCRT	2	1.4	13293	1.40	265.9
7	0°	HSNFCCRT	3	2.0	16819	2.00	336
8	-45°	HSNMCCRT	1	1.1	13281	1.10	265.6
9	+45°	HSNMCCRT	1	1.1	13281	1.10	265.6
10	0°	HSNFCCRT	3	2.0	16819	2.00	336

Table 4.2: Results under compressive loading. FI = Failure Index;  $\varepsilon$  = Strain;  $\sigma$  = Stress.

In Figure 4.3, the failure of ply 2 due to matrix compression is shown as an example. This indicates that in a subsequent simulation with a higher applied displacement, plies 2,3,8 and 9 were deactivated in the composite layup as they had already exceeded the failure criterion.

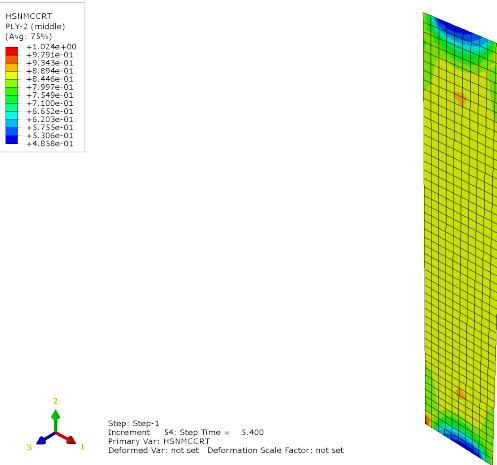


Figure 4.3: Result HSNMCCRT for ply 2.

#### 4.2.1 Failure Sequence and Interpretation

Given that the compressive load is applied along the **Y-axis**, the ply response is strongly influenced by fiber orientation and the nonlinear behaviour of composites under compression:

- **±45° plies (Plies 2, 3, 8, 9):** Fail **first** at 1.1 mm displacement and 265.6 MPa stress. These plies are angled at ±45° with respect to the loading axis, causing them to undergo in-plane shear. The dominant failure mode is matrix compression (HSNMCCRT), likely due to shear-induced damage such as matrix micro-buckling or fiber–matrix interface failure.
- **90° plies (Plies 5 and 6):** Fail **second** at 1.4 mm displacement and 265.9 MPa stress. Fibers in these plies are aligned with the loading direction and would be expected to carry compressive load. However, matrix compressive failure (HSNMCCRT) dominates again, suggesting local instability, fiber waviness, or imperfections that cause stress concentrations in the matrix.

- **$0^\circ$  plies (Plies 1, 4, 7, 10):** Fail last at 2.0 mm and 336 MPa stress. Despite their fibers being transverse to the loading direction, these plies reach the threshold for fiber compressive failure (HSNFCCRT). This implies that redistributed stresses, likely due to previous ply failures or interlaminar effects, induced sufficient compressive loading along the fiber direction to trigger catastrophic failure.

#### 4.2.2 Stress–Strain Curve Interpretation

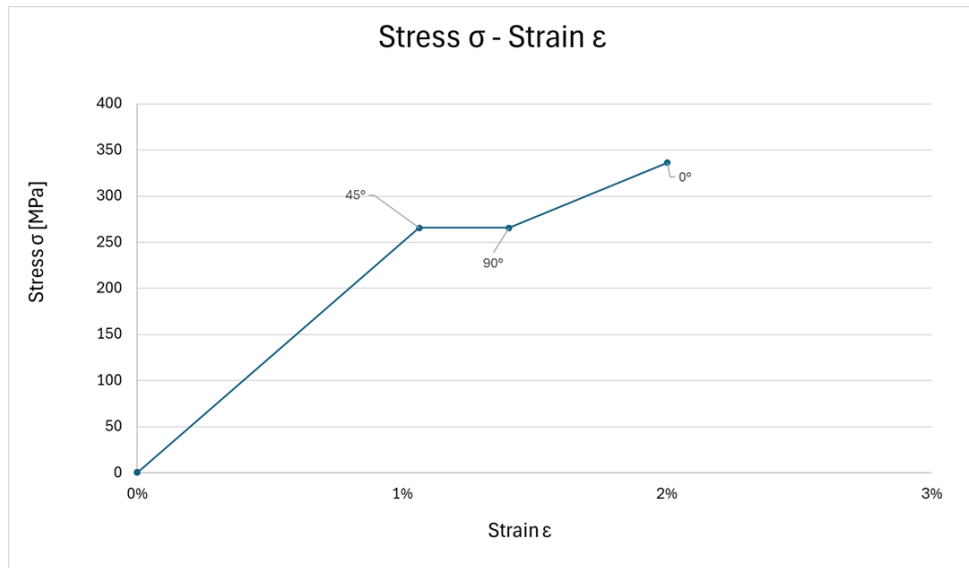


Figure 4.4: Stress–strain curve under compressive loading (Y-axis), with failure stages.

In Figure 4.4, the laminate exhibits a clear **stepwise stiffness reduction**, indicating progressive failure:

- **Point 1:** Initial drop due to  $\pm 45^\circ$  matrix shear failure.
- **Point 2:** Second drop due to  $90^\circ$  ply matrix compressive failure.
- **Point 3:** Final drop associated with fiber compressive failure in the  $0^\circ$  plies.

#### 4.2.3 Failure Mode Summary

The failure sequence ( $\pm 45^\circ \rightarrow 90^\circ \rightarrow 0^\circ$ ) under compression reflects the different mechanical responses of fiber and matrix under compressive stress.

The matrix fails first under shear and compression, allowing progressive redistribution of stress.

Final failure occurs via HSNFCCRT, confirming the onset of catastrophic compressive fiber failure in off-axis plies due to accumulated internal stress and damage evolution.

As in the tensile case, the Y-axis loading direction plays a fundamental role in defining which plies experience axial load, shear, or transverse compression — shaping the sequence and nature of failure.

# Chapter 5

## Ratio Analysis

### 5.1 Calculation of Tensile to Compressive Strength Ratio

To evaluate the performance characteristics of the composite material under different loading conditions, it is informative to calculate the ratio between its ultimate tensile strength (UTS) and ultimate compressive strength (UCS).

#### 5.1.1 Ultimate Strengths

Based on the data from the simulations:

- The ultimate tensile strength ( $\sigma_{Ut}$ ) is observed at 413 MPa, corresponding to the failure of the 0° plies.
- The ultimate compressive strength ( $\sigma_{Uc}$ ) is determined at 336 MPa, identified at the failure point of the same 0° plies under compression.

#### 5.1.2 Strength Ratio Calculation

The ratio of tensile to compressive strength ( $X$ ) can be calculated using the following formula:

$$X = \frac{\sigma_{Ut}}{\sigma_{Uc}}$$

Plugging in the values:

$$X = \frac{413 \text{ MPa}}{336 \text{ MPa}} \approx 1.23$$

#### 5.1.3 Interpretation

This ratio of 1.23 indicates that the composite material is approximately 23% stronger in tension than in compression for the same fiber orientation and loading direction. This difference may arise due to different failure mechanisms inherent to tensile and compressive loads, such as fiber buckling or kinking under compression versus fiber breaking under tension.

## 5.2 Conclusion

The calculated tensile-to-compressive strength ratio provides valuable insight into the composite's structural integrity under different stress states. A higher ratio implies that the material could be preferentially optimized or utilized in applications where tensile stresses are more prevalent than compressive ones. Understanding this ratio helps in designing more efficient and safer composite structures by tailoring the layup or material properties according to the dominant loading conditions anticipated in practical applications.